SLA determination in coastal areas using Least-Squares Collocation and Cryosat-2 data

O.N. Altiparmaki✉[1], D.A. Natsiopoulos[2], G.S. Vergos[3]

[1] GravLab, Department of Geodesy and Surveying, Aristotle University of Thessaloniki, Thessaloniki, GR-54124, Greece, (raltiparmaki@hotmail.com/+302310994366)

[2] GravLab, Department of Geodesy and Surveying, Aristotle University of Thessaloniki, Thessaloniki, GR-54124, Greece, (dnatsio@topo.auth.gr)

[3] GravLab, Department of Geodesy and Surveying, Aristotle University of Thessaloniki, Thessaloniki, GR-54124, Greece, (vergos@topo.auth.gr)

Abstract

Satellite altimetry has provided during the last 30 years an unprecedented amount of high-resolution and high-accuracy data for the state of the oceans. With the latest altimetric satellites utilizing the SAR and SAR-in modes, reliable sea surface heights close to the coastline can be determined more efficiently. The main purpose of this paper is to estimate Sea Level Anomalies (SLAs) close to the coastline and to areas where data are absent, while Least Squares Collocation (LSC) has been used to carry out the prediction. The selected study area is the entire Mediterranean Sea and the estimation of SLA values was carried out using raw Cryosat-2 observations. For LSC to be applied, empirical and analytical covariance function models are defined and evaluated for estimating SLAs within 10° block windows. In order to investigate the accuracy of the analytical covariance functions that provide the most accurate results, prediction has been carried out at a single point, randomly selected in the Greek region being close to the coastline. From the analysis carried out, three types of analytical covariance functions were deemed as the optimal ones, providing a mean prediction accuracy at the 3.7 cm level. These models were then used for the SLA estimation at the 10º windows, specifying local empirical and analytical covariance function models. The prediction accuracies achieved range between 3.7 cm and 12.5 cm depending on the presence of islands.

Keywords: Cryosat-2, least-squares collocation, sea level anomalies, coastal areas, prediction

1. Introduction

Over the last few decades, climate induced ocean variations have been one of the most important environmental problems worldwide. Taking into consideration and studying

these changes, the scientific community has tried to gather even more information about their triggering factors and their consequences. This has been largely achieved through dedicated satellite missions aiming to monitor the marine environment and the mass loss in the Polar Regions, which is caused by ice melting. One of the main consequences are increasing levels of the Earth's oceans with foreseen impact on the anthropogenic and natural environment. To that respect, and in order for satellite data to be incorporated in forecasting and assimilation models, their inherent high-accuracy over marine regions should be extended to coastal ones and to areas where data are absent. Additionally, improved representation and estimation of sea surface heights close to the coastline will have a direct, positive, impact on height system unification (HSU) in remote areas and regions where GPS-derived ellipsoidal heights cannot be acquired (Gruber et al. 2012). For the altimetric records to be extended close to the coastline an interpolation, extrapolation in reality, needs to be carried out. In that way, the continuous along-track measurements in pure sea areas will be brought closer to coastal areas and within a small distance (close to 1 km) from the coasts, where a Tide Gauge (TG) station is situated. For this prediction to be carried out accurately, a rigorous method should be employed. In physical geodesy, Least Squares Collocation (LSC) has been used for long as an optimal estimator (Barzaghi et al. 2009, Moritz 1980), in the sense that it provides highly accurate prediction results, given the data accuracy and the statistical characteristics of the input field. LSC requires knowledge of both input data and error variance-covariance matrices, the latter being defined by the analytical covariance functions of the input signals. The mission of Cryosat-2 offers dense cross-track spacing as a result of the Synthetic Aperture Radar (SAR) and SAR-in drifting modes leading to high spatial resolution (Francis 2007, Wingham et al. 2006). Due to the fact that the Mediterranean Sea is a semi-enclosed marine region with many islands and isles disrupting the pure marine observations, Cryosat-2 was chosen as the most appropriate for the specific nature of this particular study area (Andersen and Piccioni 2016). Through Cryosat-2 data, analytical covariance functions were estimated based on exponential, polynomial and Gauss-Markov models, and prediction of Sea Level Anomaly (SLA) values has been carried out to conclude on the most proper ones in order to derive SLAs in coastal areas. The analytical models providing the highest prediction accuracy are then used to extend the SLA information in areas with little or no data, especially close to the coastline. To that respect, the entire Mediterranean basin was split in individual windows of $10°\times10°$ degrees, and separate empirical covariance

functions have been estimated, in order to derive representative analytical models for each sub-area. Finally, the absolute accuracies offered by the various covariance models were assessed by comparing them as to the results they provide in a specific prediction case.

2. Satellite altimetry data availability and methodology

The used raw data refer to SLAs for one cycle (cycle 13 – 12127 SLA values) of the Cryosat-2 satellite mission from 14.03.2011 to 12.04.2011 within the entire Mediterranean Sea ($30° \leq \varphi \leq 50°$ and $-10° \leq \lambda \leq 40°$). The Cryosat-2 data were acquired from the RADS system (RADS 2016, Scharroo et al. 2013), which has a collection of data from past and current satellite altimetry missions. All geophysical and instrumental corrections have been applied, using the default models proposed by the RADS system, so that corrected SLAs would be available. During this pre-processing step, the derived SLAs have been referred to the EGM2008 Zero-Tide (ZT) geoid (Pavlis et al. 2012) and the Jason ellipsoid (Dumont et al. 2016). Figure 1 depicts the distribution of the Cryosat-2 data over the entire Mediterranean basin as well as the SLA variations, while Table 1 presents the respective statistics.

Figure 1

To evaluate the performance of SLA prediction close to the coastline, LSC has been employed using various covariance functions. Initially, in order to evaluate their performance the available data have been separated in two equal halves, one acting as the input dataset and the other as the prediction one. A bin size of 20km was chosen for the analytical covariance functions, while points up to distances of 300 km from the prediction point have been used. Initially, the empirical covariance function model was calculated in order to represent the local statistical characteristics. If each observation y_i represents a small area A_i and y_j represents an area A_j then the empirical covariance is (Tscherning and Rapp 1974):

$$C_k = \frac{\sum A_i A_j y_i y_j}{\sum A_i A_{j_k}} . \quad (1)$$

If the area is subdivided into small cells holding one observation each and *Ai* and *Aj* are assumed to be equal then Eq. (1) reduces to:

$$C_k = \frac{\sum y_i y_j}{\sum N_k}, \quad (2)$$

where N_k is the number of products $y_i\, y_j$ in the k^{th} interval (Knudsen 1987). In our case the empirical covariances of SLA (h^{SLA}) for a given spherical distance ψ is:

$$C_k = (h_i^{SLA}, h_j^{SLA}, \psi) = M\{h_i^{SLA}, h_j^{SLA}\}_\psi . \quad (3)$$

where $M\{h_i^{SLA}, h_j^{SLA}\}_\psi$ is the mean value of products between h_i^{SLA} and h_j^{SLA} which are included in the bin size of 20km.

The analytical covariance function models employed have been based on four exponential, one polynomial and two Gauss-Markov models (Natsiopoulos et al. 2016, Vergos et al. 2013), as:

$$C_{h^{SLA}h^{SLA}}(\psi) = a\mathrm{e}^{(b\psi)} + c\mathrm{e}^{(d\psi)}, \quad (4)$$

$$C_{h^{SLA}h^{SLA}}(\psi) = a\mathrm{e}^{(-b\psi^2 - c\psi)}, \quad (5)$$

$$C_{h^{SLA}h^{SLA}}(\psi) = a\mathrm{e}^{(-(\psi/b)^2)} + c\mathrm{e}^{(-((\psi-d)/u)^2)}, \quad (6)$$

$$C_{h^{SLA}h^{SLA}}(\psi) = a\mathrm{e}^{(-b\psi)}\cos(c\psi), \quad (7)$$

$$C_{h^{SLA}h^{SLA}}(\psi) = a\psi^3 + b\psi^2 + c\psi + d . \quad (8)$$

In Eqs. (4) - (8), *a*, *b*, *c* and *d* denote parameters to be determined, so that the analytical covariance model will fit the empirical one, ψ is the spherical distance and $\psi_{k-1} < \psi_{ij} < \psi_k$. The 2nd and 3rd order Gauss-Markov models are outlined in Eqs. (9) and (10) respectively, where *D* is the characteristic distance, *r* is the planar distance and $\sigma^2_{h^{SLA}}$ the SLA variance (Jordan 1972; Knudsen and Tscherning 2007):

$$C_{h^{SLA}h^{SLA}}(r) = \sigma^2_{h^{SLA}}(1 + \frac{r}{D})e^{(-\frac{r}{D})}, \quad (9)$$

$$C_{h^{SLA}h^{SLA}}(r) = \sigma^2_{h^{SLA}}(1 + \frac{r}{D} + \frac{r^2}{3D^2})e^{(-\frac{r}{D})}. \quad (10)$$

The above models are represented as model A, B,…,G in the following tables, in order to make it easier to read. The estimation is carried out as (Knudsen and Tscherning, 2007; Tscherning and Rapp, 1974):

$$\boldsymbol{h}^{SLA}(P) = \boldsymbol{C}_{h^{SLA}h^{SLA}}(P,\square)\boldsymbol{C}^{-1}_{h^{SLA}h^{SLA}}\boldsymbol{h}^{SLA} \quad (11)$$

In Eq. (11), $\boldsymbol{h}^{SLA}(P)$ denotes the SLA to be predicted at point P, $\boldsymbol{h}^{SLA}$ is the vector of observations, $\boldsymbol{C}_{h^{SLA}h^{SLA}}(P,\cdot)$ is the cross-covariance matrix between the SLA to be predicted and the input signals and $\boldsymbol{C}^{-1}_{h^{SLA}h^{SLA}}$ is the full variance-covariance matrix of the input SLA determined from the used analytical covariance function model**.**

3. Numerical results for Mediterranean Sea

In the sequel, the results from the evaluation of alternative analytical covariance function models are presented. Table 1 presents the statistics of the initial SLA dataset and its differences with the predicted ones using the aforementioned analytical covariance function models. From Table 1 it can be seen that the accuracy of SLA values is improved using LSC method, as indicators precision are taken into account at original ones. All models present a mean value close to zero, whereas simultaneously the exponential models A and D and the polynomial model E provide the optimum results with a std at the 3.70 cm, 3.72 cm and 3.69 cm respectively. The exponential model B provides a std at the 3.76 cm, which can also be accepted for a subsequent prediction. In this paper were chosen the three optimum models for further investigation. The 2nd and 3rd order Gauss Markov models provide a std at the 8.38 cm and 5.44 cm respectively, which can be considered as larger compared to that of the exponential and polynomial models. The exponential model C presents the worst fitting at initial data with a std at the 60.60 cm, both in open sea and close to coastline.

Table 1

Models A, D and E were then chosen to carry-out SLA estimation close to the coastline. In order to predict those SLA values with high prediction accuracy, the input data were separated in 10 windows each spanning 10° (see Figure 2). The concept is that locally estimated analytical covariance functions will depict the SLA variability better compared to a global Mediterranean-wide one. The estimation was carried-out to specific points up to a radius of 100 km from the coastline. From this set of points, those within a distance of 15 km from the coastline were the prediction ones, whereas those between 16 km and 100 km were the ones acting as the input since they are located in the open water. This scenario resembles the case where altimetry data are available in purely marine areas and they need to be interpolated and/or extended close to the coastline. Table 2, presents the statistics of the differences between the original SLAs and those predicted with the chosen analytical covariance function models A, D and E.

Figure 2

From above table, it can be seen that using LSC SLA prediction is carried out with reasonable accuracy in all windows except windows 8 and 10. In window 8 an initial std at the 11.20 cm was calculated, whereas for the exponential model A the accuracy is at the 5.13 m, which indicates that this model does not fit well to the dataset. Model E in the same window provides also a worse std compared to the initial values at the 15.30 cm, whereas the exponential model D provides a std at the 7.70 cm, which can be considered as acceptable, despite the fact that it is at the almost equal to the input std. In window 10 the SLA has a std of 22.32 cm, while model E provides a prediction accuracy of 26.66 cm. Model A and Model D provide a better std than that of the initial one at the 8.65 cm and 8.64 cm respectively. The optimum prediction accuracy is achieved for window 3 and specifically for the polynomial model E at the 3.63 cm, which is smaller by 63% compared to the error of the input data, if one considers the std as an indication of the variability of the input field. Models A and D in the same window present also high prediction accuracy at the 4.47 cm and 3.71 cm respectively. The same behavior is also see for window 2 with a std at the 3.98 cm, 3.97 cm and 3.88 cm for Models A, D and E, respectively. In window 4 the SLA has a std of 12.71 cm

and the prediction accuracy reaches 7.05 cm, 6.66 cm and 7.09 for model A, D and E respectively. Window 5 presents slightly worse prediction accuracy at the 8.80 cm, 7.29 cm and 7.89 cm. For window 1, polynomial model E presents the best results at the 7.76 cm compared to the others optimum models A and D in the same window which provide a std at the 11.81 cm and 12.09 cm respectively. This worst performance by almost 4 cm is seen for window 6 as well, in which the exponential model A provides a std at the 8.80 cm, whereas exponential model D and polynomial model E give 12.18 cm and 12.10 cm respectively. Windows 7 and 9 provide results with a std more than 10 cm, but simultaneously better than that of initial ones. Specifically, window 7 presents a std at the 12.38 cm, 12.45 cm and 12.10 cm and window 9 provides a std at the 11.90 cm, 11.88 cm and 15.28 cm for the three optimum models A, D and E respectively. From the above results it can be concluded that the highest std is provided by the prediction windows with good distribution of points, that act as the input data for the calculation of analytical covariance functions, around the prediction points. For example, window 5 presents for the exponential model A a std smaller by 40% compared to the corresponding model in window 9, for exponential model D a std smaller by 44% and for polynomial model E a std smaller by 54%.

Table 2

In order to evaluate the three optimum analytical covariance function model and different scenarios for the distribution of the input data, a point was randomly selected for a Greek area close to coastline (see Figure 3). The above prediction strategy was carried out once more, utilizing three different approaches concerning the distribution of points which act as the input data for the calculation of the analytical covariance functions and the prediction. Table 3, presents the differences between the original SLAs and those predicted from the three alternative scenarios. For the first test, all points within window 4, where the estimation point is located, were chosen. For the second test a window of 2° (~220 km) around the estimation point was chosen and for the third test all points within the entire Mediterranean basin were taken into account.

Figure 3

Table 3

From Table 3 it can be seen that model D provides the smallest differences for all three scenarios. Specifically, for Model A the best results are given from scenario 2 with a difference at 0.15 cm. Scenario 1 and 3 provide a difference at the 2.8 cm and 3.23 cm respectively. Exponential model D presents differences less at the 0.03 cm, 0.04 cm and 0.09 cm level with the optimal results being achieved when the points located in the immediate vicinity of the prediction point are considered. Polynomial Model E gives also good results at the 0.14 cm, 0.09 cm and 0.35 cm. From the above we can conclude that scenario 2 gives the best results for this test case. This is due to the fact that only points around a small region of the prediction point were taken into account for the calculation of the analytical covariance functions, so that only the local variability of the LSA around the prediction point is considered, therefore within a radius of ~220 km. In general, it will differ depending on the area extent around the prediction point and the amount of data within it, as well as on the quality of the sea level anomalies given proximity to land. Further statistical tests are needed for the bounds of the data used in the analytical function computation, as this case is based on the prediction of only one point.

4. Conclusions

A preliminary estimation of SLA values in the entire Mediterranean Sea was carried out using LSC and Cryosat-2 data, with the aim to investigate prediction errors in coast areas. Seven analytical covariance functions were evaluated and the three best of these, i.e., Models A, D and E, were then used for the re-estimation of SLA values at points within a distance of 15 km from the coastline. The study area was separated at 10 windows each spanning 10° and locally estimated analytical covariance functions were calculated with the purpose to depict better the SLA variability compared to a global Mediterranean-wide covariance function. The higher prediction accuracy was achieved at the windows in which there are many data with good spatial distribution. In order to further investigate the performance of the optimum models, a point was randomly selected in the Aegean Sea close to the coastline. Then, three different scenarios of input data availability and distribution were evaluated. It was concluded that LSC provides high accuracy for the prediction of SLA values in areas with little or no data, especially close to the coastline, with an optimal selection radius of 220 km around the

prediction point. The selection radius is based on the results of the present scenario set-up and can vary in other areas given sea/land setup and data availability. In that case, a sub-cm prediction accuracy can be achieved, with obvious applications in extending the sea level altimetry records from open sea to coastal areas.

References

Andersen OB, Piccioni G (2016) Recent Arctic Sea Level Variations from Satellites. Front Mar Sci 3:76. doi: 10.3389/fmars.2016.00076.

Barzaghi R, Tselfes N, Tziavos IN, Vergos GS (2009) Geoid and High Resolution Sea Surface Topography Modelling in the Mediterranean from Gravimetry, Altimetry and GOCE Data: Evaluation by Simulation. Journal of Geodesy 83(8):751-772. doi: 10.1007/s00190-008-0292-z.

Dumont JP, Rosmorduc V, Carrere L, Picot N, Bronner E, Couhert A, Guillot A, Desai, S, Bonekamp, H, Figa J, Scharroo R, Lillibridge J (2016) Jason-3 Products Handbook, SALP-MU-M-OP-16118-CN.

Francis CR (2007) CryoSat Mission and Data Description. CS-RP-ESA-SY-0059, ESTEC Noordwijk, The Netherlands.

Gruber T, Gerlach C, Haagmans R (2012) Intercontinental height datum connection with GOCE and GPS-levelling data. J Geod Scien 2(4): 270-280, doi:10.2478/v10156-012-0001-y.

Jordan SK (1972) Self-Consistent Statistical Models for the Gravity Anomaly, Vertical Deflections, and Undulation of the Geoid. J Geophys Res **77(20)**: 3660-3670.

Knudsen P (1987) Estimation and modelling of the local empirical covariance function using gravity and satellite altimeter data. Bull Geod 61:45-160.

Knudsen P and Tscherning CC (2007) Error Characteristics of dynamic topography models derived from altimetry and GOCE Gravimetry. In: Tregoning P and Rizos C (eds) IAG Symposia "Dynamic Planet 2005 - Monitoring and Understanding a Dynamic Planet with Geodetic and Oceanographic Tools" Vol 130, Springer Berlin Heidelberg, 11-16. doi: 10.1007/978-3-540-49350-1_2.

Moritz H (1980) Advanced Physical Geodesy, second ed. Wichmann, Karlsruhe.

Natsiopoulos DA, Vergos GS, Tziavos IN, Grigoriadis VN (2016) Sea level variability in the Mediterranean Sea through satellite altimetry analytical covariance functions. Rossikopoulos D, Fotiou A, Paraschakis I (eds) Special Issue dedicated to the Emeritus Professor Christogeorgis Kaltsikis, Ziti Editions, pp. 327-347.

Pavlis NK, Holmes SA, Kenyon SC, Factor JK (2012) The Development and Evaluation of the Earth Gravitational Model 2008 (EGM2008). J Geophys Res 117(B04406), doi:10.1029/2011JB008916.

RADS (2016) Available from: http://rads.tudelft.nl (Radar Altimeter Database System). Accessed May 2016.

Scharroo R, Leuliette EW, Lillibridge JL, Byrne D, Naeije MC, Mitchum GT (2013) RADS: Consistent multi-mission products. European Space Agency "20 Years of progress in radar altimetry", ESA Publications SP-710.

Tscherning C.C. and Rapp R.H., 1974. Closed covariance expressions for gravity anomalies, geoid undulations, and deflections of the vertical implied by anomaly degreevariance

290 models. Reports of the Department of Geodetic Science, 208. The Ohio State
291 University, Columbus, Ohio.

292 Vergos GS, Natsiopoulos DA, Tziavos IN (2013) Sea level anomaly and dynamic ocean
293 topography analytical covariance functions in the Mediterranean Sea from ENVISAT
294 data. European Space Agency “20 Years of progress in radar altimetry”, ESA
295 Publications SP-710.

296 Wingham D, Francis C, Baker S, Bouzinac C, Brockley D, Cullen R, de Chateau-Thierry P,
297 Laxon S, Mallow U, Mavrocordatos U, Phalippou L, Ratier G, Rey L, Rostan F, Viau P,
298 Wallis D (2006) CryoSat: a mission to determine the fluctuations in Earths land and
299 marine ice fields. Adv Space Res 37:841–871. doi: 10.1016/j.asr.2005.07.027.

300

Table 1: Statistics of the original SLAs and differences with the predictions based on the various covariance function models. Units: [cm]

	Initial	Model A	Model B	Model C	Model D	Model E	Model F	Model G
min	-100.0	-42.4	-44.0	-3345.1	-42.0	-42.1	-224.3	-146.8
max	67.9	50.2	50.6	1740.0	50.2	50.2	218.2	135.4
mean	-11.8	0.0	-0.1	0.1	0.0	0.0	0.1	0.1
std	17.1	3.7	3.8	60.6	3.7	3.7	8.4	5.4
rms	20.8	3.7	3.8	60.6	3.7	3.7	8.4	5.4

Table 2: Statistics of initial SLAs and differences with the estimated ones for all 10 windows (pts: points). Unit [cm]

1 [87 pts]	Initial	Model A	Model D	Model E	6 [70 pts]	Initial	Model A	Model D	Model E
min	-47.6	-33.4	-35.1	-24.0	min	-90.1	-27.1	-66.4	-64.9
max	35.5	37.8	37.7	37.8	max	29.4	26.8	22.9	23.1
mean	-8.3	-4.3	-4.4	-1.1	mean	-5.4	-1.8	1.0	1.2
std	19.4	11.8	12.1	7.8	std	18.9	8.8	12.2	12.1
rms	21.1	12.6	12.9	7.8	rms	19.6	9.0	12.2	12.2
2 [53 pts]	**Initial**	**Model A**	**Model D**	**Model E**	**7 [41 pts]**	**Initial**	**Model A**	**Model D**	**Model E**
min	-38.6	-9.0	-9.2	-9.1	min	-101.6	-68.9	-68.9	-64.9
max	-3.1	10.2	10.8	10.8	max	-7.5	14.9	17.5	23.1
mean	-24.4	1.5	1.4	1.4	mean	-34.6	-3.9	-3.7	1.2
std	8.5	4.0	4.0	3.9	std	15.2	12.4	12.5	12.1
rms	25.8	4.3	4.2	4.1	rms	37.8	13.0	13.0	12.2
3 [70 pts]	**Initial**	**Model A**	**Model D**	**Model E**	**8 [80 pts]**	**Initial**	**Model A**	**Model D**	**Model E**
min	-38.6	-10.5	-11.8	-11.3	min	-49.8	-3593.5	-34.6	-93.1
max	9.1	8.1	9.0	7.6	max	7.9	9.2	11.3	13.8
mean	-16.2	0.6	0.3	0.2	mean	-24.5	-129.4	-3.6	-6.2
std	10.2	4.5	3.7	3.6	std	11.2	513.1	7.7	15.3
rms	19.1	4.5	3.7	3.6	rms	27.0	529.2	8.5	16.5
4 [172 pts]	**Initial**	**Model A**	**Model D**	**Model E**	**9 [29 pts]**	**Initial**	**Model A**	**Model D**	**Model E**
min	-73.1	-40.3	-22.9	-26.1	min	-100.0	-11.3	-9.0	-93.1
max	6.9	22.7	34.9	32.3	max	67.8	45.6	47.6	13.8
mean	-20.8	-2.1	-0.8	-0.9	mean	-5.6	2.2	2.3	-6.2
std	12.7	7.1	6.7	7.1	std	31.5	11.9	11.9	15.3
rms	24.3	7.4	6.7	7.1	rms	32.0	12.1	12.1	16.5
5 [41 pts]	**Initial**	**Model A**	**Model D**	**Model E**	**10 [91 pts]**	**Initial**	**Model A**	**Model D**	**Model E**
min	-49.2	-27.1	-17.1	-17.8	min	-42.6	-41.0	-40.9	-122.1
max	23.2	26.8	20.0	19.5	max	70.7	24.1	24.0	41.0
mean	-17.7	-1.8	-0.2	0.4	mean	19.8	2.1	2.1	-1.7
std	14.6	8.8	7.3	7.9	std	22.3	8.7	8.6	26.7
rms	22.9	9.0	7.3	7.9	rms	29.8	8.9	8.9	26.7

311 **Table 3:** Differences between the original altimetry SLA value and the estimated ones for three
312 alternative scenarios. Unit [cm]

Point Code	latitude (°)		longitude (°)		Initial SLA value (cm)	
7287	37.569032		26.689857		-26.80	
	SLA estimation	Difference (1)	SLA estimation	Difference (2)	SLA estimation	Difference (3)
Model A	-24.0	-2.8	-27.0	-0.2	-23.6	-3.2
Model D	-26.8	0.0	-26.8	0.0	-26.9	-0.1
Model E	-26.7	-0.1	-26.9	-0.1	-26.5	-0.4

313

314

315 **Figure 1:** Cryosat-2 cycle 13 data distribution over the entire Mediterranean Sea

316 **Figure 2:** Satellite altimetry data availability at a radius of 15 km (red) and 85 km (green) from

317 the coastline within the 10°×10° windows

318 **Figure 3:** Cryosat-2 data availability around the prediction point

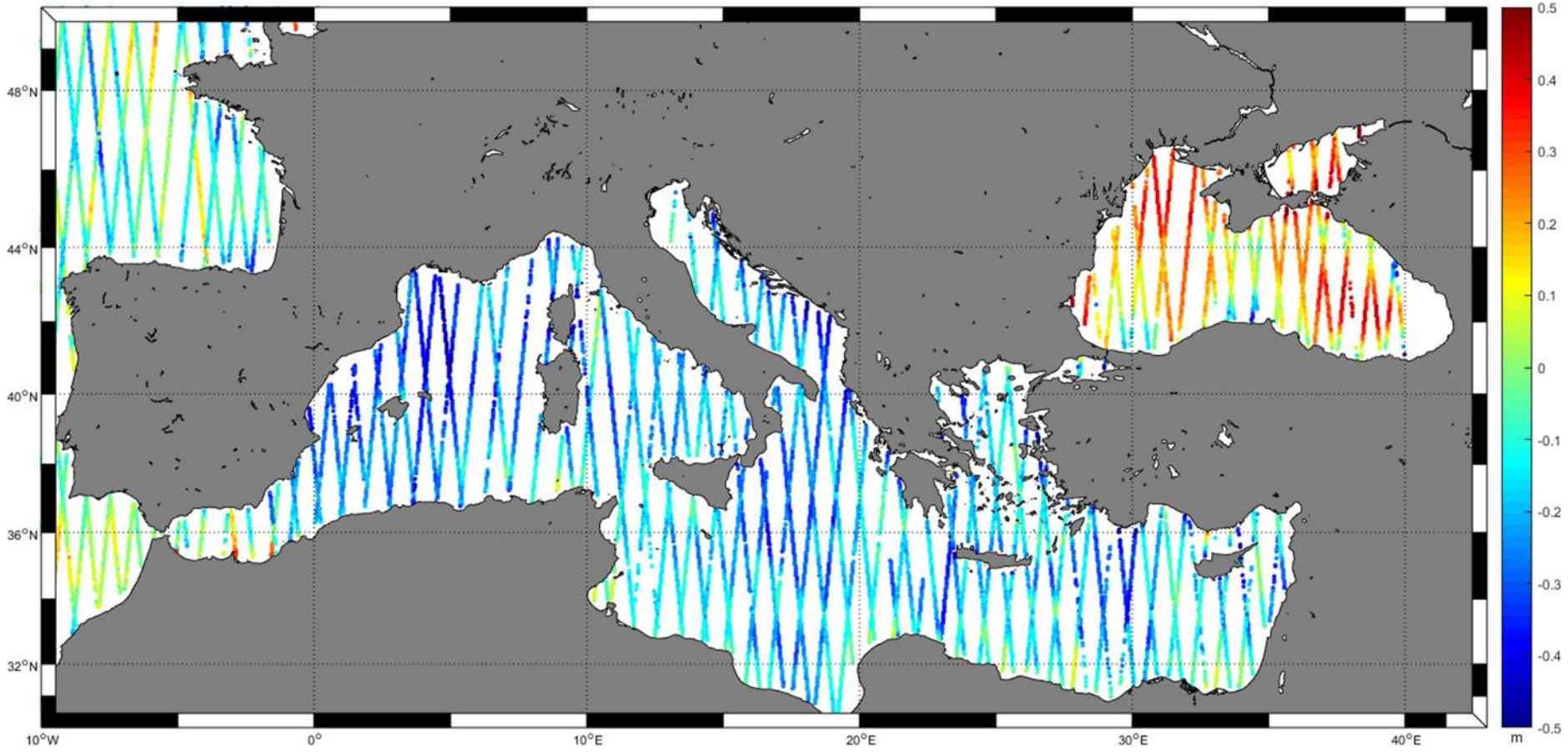
48°N
44°N
40°N
36°N
32°N
10°W
0°
10°E
20°E
30°E
40°E
0.5
0.4
0.3
0.2
0.1
0
-0.1
-0.2
-0.3
-0.4
-0.5
m

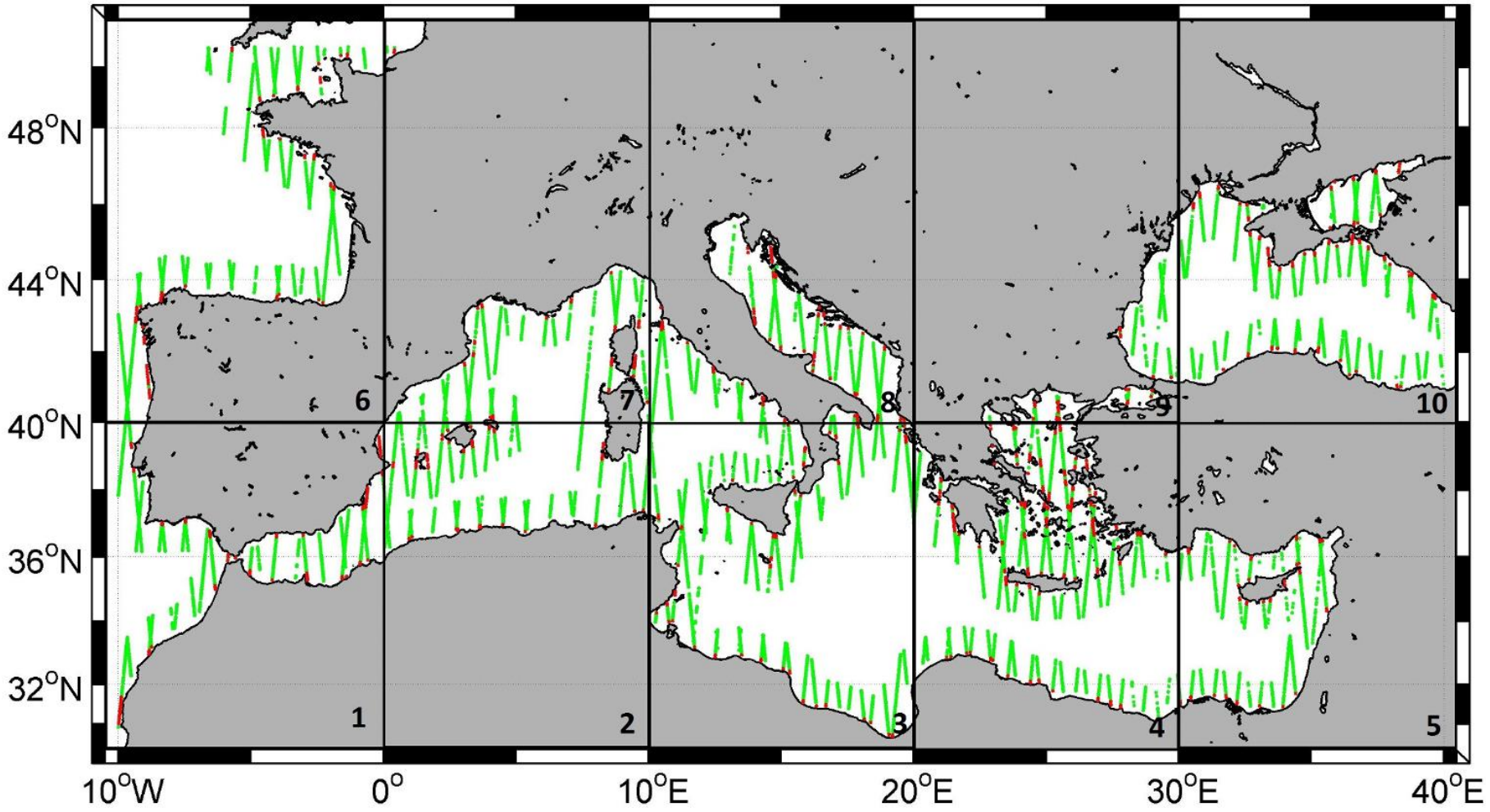

321

322

323

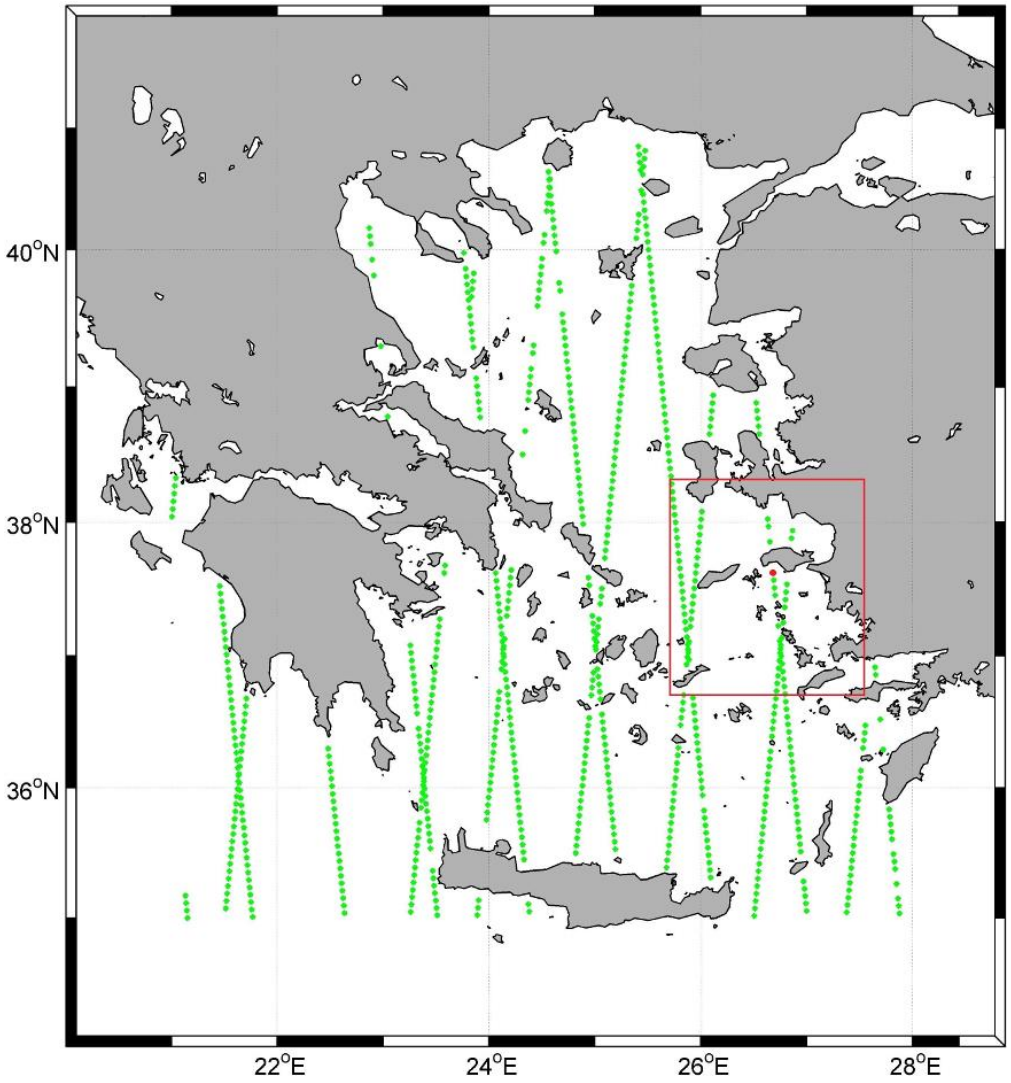
40°N
38°N
36°N
22°E
24°E
26°E
28°E